Photochemistry

DOI: 10.1002/ange.201107467

The Influence of Oxygen Content on the Thermal Activation of Hematite Nanowires**

*Yichuan Ling, Gongming Wang, Jay Reddy, Changchun Wang, Jin Z. Zhang, and Yat Li**

A promising photoelectrode material for solar-driven water splitting, hematite (α-Fe_2O_3) is non-toxic, abundant, chemically stable, low-cost, and has a bandgap of approximately 2.1 eV,[1–5] which accounts for a maximum theoretical solar-to-hydrogen (STH) efficiency of 15%.[4] This last property compares favorably with the most studied metal oxide materials for photoeletrochemical (PEC) water splitting, including TiO_2,[6–10] ZnO,[11] and WO_3.[12–15] However, the reported STH efficiencies of hematite photoelectrodes are substantially lower than the theoretical value, owing to several limiting factors such as poor conductivity, short excited-state lifetime (<10 ps),[16] poor oxygen evolution reaction kinetics,[17] low absorption coefficient,[18] short diffusion length for holes (2–4 nm),[19] and lower flat-band potential in energy for water splitting.[4,20] Enormous efforts have been made to overcome these limitations of hematite, including the incorporation of oxygen evolving catalysts to reduce the kinetic barrier for water oxidation on the hematite surface,[21–23] the development of nanostructures to increase the effective surface area and to reduce diffusion length for carriers,[4,5,24] as well as the development of element-doped hematite for improving electrical conductivity and/or light absorption.[2]

Recently, we demonstrated that TiO_2 nanowires thermally treated in hydrogen showed increased donor density and PEC performance as a result of the formation of oxygen vacancies.[6] We anticipated that creating oxygen vacancy (V_O), and thereby Fe^{2+}, sites in hematite could significantly increase the conductivity of the material through a polaron hopping mechanism.[25,26] Although V_O can be created by sintering hematite in a reductive atmosphere such as hydrogen, it may introduce hydrogen as a dopant into the structure. Additionally, hematite can be easily reduced in hydrogen to produce magnetite (Fe_3O_4), which is photo-inactive.[27] Herein, we report an alternative method for the preparation of highly conductive and photoactive hematite through thermal decomposition of β-FeOOH in an oxygen-deficient atmosphere (N_2 + air). The resulting hematite sample showed substantially enhanced photoactivity compared to the pristine hematite prepared in air. The oxygen content during thermal activation significantly affects the formation of V_O and thereby the photoactivity of hematite nanowires for water oxidation. This is the first demonstration of highly photoactive hematite nanowire arrays at a relatively low activation temperature without a dopant element.

Akaganeite nanowires were prepared through the hydrolysis of $FeCl_3$ (0.15 M) in an environment with a high ionic strength (1 M $NaNO_3$) and low pH value (pH 1.5, adjusted by HCl) at 95°C for 4 h.[28] The resulting yellow film on a fluorine-doped tin oxide (FTO) substrate was covered with nanowire arrays with an average diameter and length of 70 nm and 700 nm, respectively (Figure 1a). X-ray diffraction

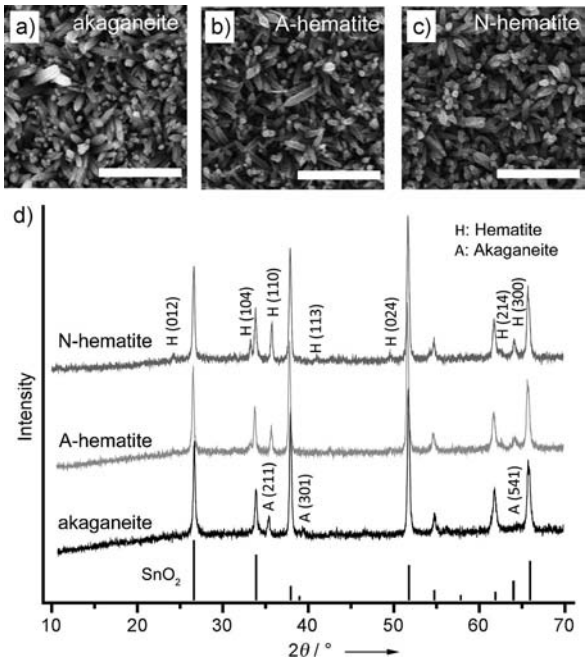

Figure 1. SEM images of a) akaganeite nanowire arrays, b) hematite nanowire arrays annealed in air, and c) hematite nanowire arrays annealed in N_2 + air. Samples (b) and (c) annealed at 550°C. Scale bars are 1 μm. d) Corresponding XRD spectra collected for akaganeite and hematite samples. Diffraction peaks for hematite (JCPDS 33-0664) and akaganeite (JCPDS 75-1594) are labeled with H(hkl) and A(hkl), respectively. The lines at the bottom indicate the diffraction peaks of SnO_2 (JCPDS 41-1445) from the FTO substrate.

[*] Y. Ling, G. Wang, J. Reddy, Prof. J. Z. Zhang, Prof. Y. Li
Department of Chemistry and Biochemistry
University of California, Santa Cruz
Santa Cruz, CA 95064 (USA)
E-mail: yli@chemistry.ucsc.edu
Prof. C. Wang
Department of Macromolecular Science and Laboratory of Advanced Materials, Fudan University, Key Laboratory of Molecular Engineering of Polymer (Minister of Education)
Shanghai, 200433 (P. R. China)

[**] Y.L. acknowledges the financial support of this work in part by NSF (DMR-0847786) and faculty startup funds granted by the University of California, Santa Cruz. Y.L. thanks the UCSC MACS Facility at Ames Research Center in Silicon Valley. We thank Honghan Fei for XRD measurements. J.Z.Z. thanks the BES Division of the U.S. DOE (DE-FG02-ER46232) for financial support. J.R. thanks the UCSC Science Internship Program and The Harker School. C.C.W. thanks the NSFC (21034003) and the Shanghai Committee of Science and Technology, China (10XD1400500) for financial support.

(XRD) analysis (Figure 1d) confirms that the nanowires are β-FeOOH (akaganeite, JCPDS 75-1594). The akaganeite-coated substrate was then washed with deionized water and sintered in an oxygen-deficient atmosphere (N_2 + air) at 550 °C for 2 h to convert akaganeite into hematite containing oxygen vacancies (N-hematite). The oxygen-deficient atmosphere was achieved by applying vacuum to the system down to a pressure of 15 Torr, and refilling with ultrahigh purity N_2 (99.998 %, Praxair). The initial oxygen content is estimated to be 0.43 % ($O_2/(O_2+N_2)\times 100\,\%$). Hematite nanowire samples (A-hematite) were prepared by sintering the akaganeite film in air at 550 °C for 2 h, as a control. Thermal activation did not change the nanowire morphology (Figure 1b,c). XRD spectra collected for both samples confirmed that the akaganeite nanowires are completely converted into hematite (JCPDS 33-0664; Figure 1d). The strongest (110) diffraction peak indicates that these hematite nanowire arrays have a preferred [110] direction on the substrate, which implies that they were grown along the [110] axis. It has been reported that the conductivity of hematite along the [110] axis is four orders of magnitude higher than the [001] direction because of a hopping mechanism related to Fe^{2+}/Fe^{3+} mixed valence states.[26]

The PEC performance of these hematite photoanodes was measured in a deaerated (purged with N_2) electrochemical cell containing a coiled Pt wire counter-electrode and a Ag/AgCl reference electrode, and using NaOH solution (1 M, pH 13.6) as the electrolyte. The measured potentials vs. Ag/AgCl were converted to the reversible hydrogen electrode (RHE) scale according to the Nernst equation:

$$E_{RHE} = E_{Ag/AgCl} + 0.059\,pH + E^{o}_{Ag/AgCl} \quad (1)$$

where E_{RHE} is the converted potential vs. RHE, $E^{o}_{Ag/AgCl} = 0.1976$ V at 25 °C, and $E_{Ag/AgCl}$ is the experimentally measured potential against the Ag/AgCl reference electrode. As shown in Figure 2, the A-hematite sample (prepared in air) yields a minimal photocurrent density in the potential range we studied and under 100 mW cm^{-2} illumination. This is consistent with previous results reported by our group and others, in which a high temperature between 650 and 800 °C is typically required for activating these hematite samples to achieve reasonable photoactivity.[2,19,29] In contrast, the N-hematite sample (prepared in N_2 + air) shows pronounced photoactivity. It yields a photocurrent density of 1.82 mA cm^{-2} at 1.23 V vs. RHE, and achieved a maximum value of 3.37 mA cm^{-2} at 1.50 V vs. RHE (Figure 2a). To our knowledge, this is the best photocurrent density ever achieved by a photoanode based on an undoped hematite nanowire. Furthermore, we have performed amperometric *I–t* studies, at an applied voltage of 1.5 V vs. RHE at 100 mW cm^{-2}, to examine the photoresponse of N-hematite over time. As shown in Figure S1 (see the Supporting Information), the photocurrent density of N-hematite is stable in a NaOH electrolyte solution (pH 13.6) for at least one hour. The onset potential is about 1.0 V vs. RHE, which is similar to other hematite photoanodes sintered at a similar temperature without oxygen-evolving catalysts.[4,30] The onset potential of N-hematite dark current is slightly shifted to higher potential, which could be because of the increased overpotential resulting from increased oxygen vacancies (Fe^{2+} sites) on the surface of the N-hematite photoanode, as compared to that of the A-hematite. Fe^{2+} sites serve as recombination centers for photoexcited holes, which could increase the overpotential for water oxidation.[31,32]

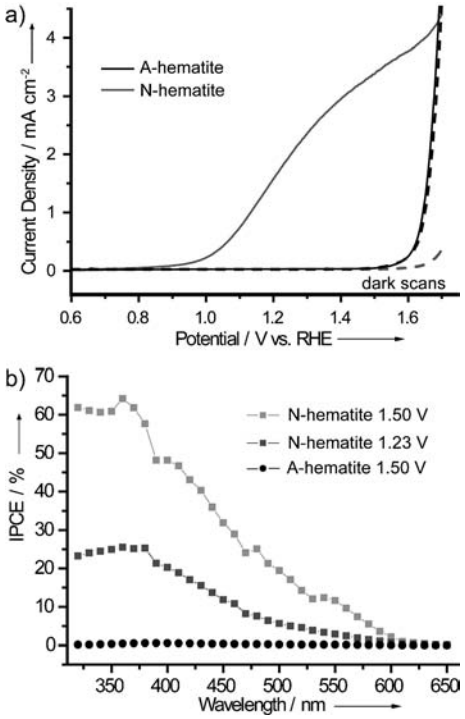

Figure 2. a) Linear sweep voltammograms collected for A-hematite (black lines) and N-hematite (gray lines), at a scan rate of 10 mV s^{-1}, in a NaOH electrolyte solution (1 M, pH 13.6) under illumination by simulated solar light of 100 mW cm^{-2} (——) and in the dark (-----). b) Corresponding IPCE spectra for A-hematite (●——) and N-hematite (■——), collected at potentials of 1.23 and 1.50 V vs. RHE (dark gray and light gray, respectively).

Incident photon-to-current conversion efficiencies (IPCE) collected for hematite photoanodes as a function of wavelength under bias at 1.23 and 1.50 V vs. RHE are shown in Figure 2b. IPCE values were calculated from the photocurrent densities obtained under different wavelengths in a range from 320 to 650 nm, and expressed as the following equation:

$$IPCE = (1240\,I)/(\lambda J_{light}) \quad (2)$$

where I (mA cm^{-2}) is the photocurrent density, λ (nm) is the incident wavelength, and J_{light} (mW cm^{-2}) is the power density of irradiance at a specific wavelength. The IPCE for A-hematite measured at 1.50 V vs. RHE is 0.57 % at 390 nm, which is consistent with its minimal photocurrent. N-hematite shows significantly enhanced IPCE values over all wavelengths (320–650 nm). The sample yields maximum IPCE values of 26 % and 64 % at 360 nm, measured at 1.23 V and 1.50 V vs. RHE, respectively. IPCE values gradually drop to zero at wavelengths above 610 nm, in accordance with the bandgap of hematite. To verify and correct a possible discrepancy in incident light profile between our xenon lamp setup (see the Experimental Section in the Supporting

Information) and the standard global solar light (AM 1.5G, 100 mW cm^{-2}), we integrated the IPCE spectra of N-hematite with a standard AM 1.5G spectral irradiance (ASTM G-173-03). The photocurrent density I measured at 1.5 V vs. RHE was calculated according to the following equation:

$$I = \int_{320}^{650} \mathrm{IPCE}(\lambda)E(\lambda)\mathrm{d}\lambda = 3.11\ \mathrm{mA\,cm^{-2}} \quad (3)$$

where $E(\lambda)$ is the solar spectral irradiance at a specific wavelength (λ) and IPCE(λ) is the obtained IPCE profile of hematite sample as a function of wavelengths (λ) at 1.50 V vs. RHE (Supporting Information, Figure S2). The calculated photocurrent, 3.11 mA cm^{-2}, is only slightly smaller than the value of 3.37 mA cm^{-2} obtained experimentally by PEC measurement (Figure 2a) at 1.50 V vs. RHE. It shows that the discrepancy from the mismatch between the simulated light used in the PEC experiments and the standard AM 1.5G solar spectrum is minor. Importantly, the PEC results unambiguously show that thermal activation of akaganeite nanowire arrays in an oxygen-deficient atmosphere (N_2 + air) at 550 °C is a simple and effective means to prepare high-performance hematite for water oxidation.

Understanding the mechanism of photoactivity enhancement is important for the design and fabrication of hematite photoanodes. Structural analysis confirms that there is no obvious difference in morphology or crystal phase for hematite nanowires prepared in the two environments (Figure 1). The enhanced photocurrent in N-hematite (vs. A-hematite) is believed to be because of the improved conductivity resulting from the creation of V_O by annealing the sample in an oxygen-deficient atmosphere. V_O is known to be a shallow donor for hematite.[3] To investigate the carrier densities of hematite samples, their electrochemical impedance values were measured in the dark at a frequency of 10 kHz. Mott–Schottky plots were generated based on the capacitances derived from the electrochemical impedance obtained at each potential (Figure 3a), in which the flat-band potential (V_{FB}) and the donor density (N_d) can be estimated. The V_{FB} for A-hematite and N-hematite were determined to be 0.41 and 0.36 V vs. RHE, respectively, which is consistent with the literature values for hematite.[25] Their N_d can be determined from the Mott–Schottky equation:

$$N_d = (2/e_0\varepsilon\varepsilon_0)[\mathrm{d}(1/C^2)/\mathrm{d}V]^{-1} \quad (4)$$

where e_0 is the electron charge (1.602×10^{-19} C) ε is the dielectric constant of hematite (80),[18] ε_0 is the permittivity of vacuum (8.854×10^{-12} F m^{-1}), and C is the capacitance derived from the electrochemical impedance obtained at each potential (V) with 10 kHz frequency in the dark. The donor density of the N-hematite was calculated to be 3.65×10^{20} cm^{-3}, which is an order of magnitude higher than that of A-hematite (3.34×10^{19} cm^{-3}). The increased donor density improves the conductivity, and thereby the collection efficiency of photo-excited electrons.

Although the synthetic method for N-hematite does not involve dopant, the enhanced donor density is expected to result from the creation of V_O during thermal activation in an oxygen-deficient environment. To verify this hypothesis, we measured Fe 2p core-level X-ray photoelectron spectroscopy (XPS) spectra for N- and A-hematite as well as their difference spectrum (Figure 3b). The Fe $2p_{3/2}$ peaks of both samples are centered at binding energies of about 711.4 eV, which is a typical value for Fe^{3+} in Fe_2O_3 and Fe_3O_4.[33–35] The binding energy is not compatible with that of FeO.[36] A satellite peak of the Fe $2p_{3/2}$ main line is observed in both samples at approximately 719 eV. This satellite is most likely indicative of the presence of a Fe^{3+} species.[29] Importantly, there is no evidence to support the presence of Fe^{2+} in A-hematite, which should give rise to a satellite peak located at 716 eV.[33] In contrast, the N-hematite sample exhibits an obvious satellite peak around 716 eV, which corresponds to Fe^{2+} (Figure 3b).[33] The results suggest that Fe^{2+} sites (V_O) were created in N-hematite. Fe^{2+} (V_O) sites act as shallow donors and therefore increase the donor density of hematite,[37] which is supported by the Mott–Schottky analysis. Furthermore, valence band spectra of A- and N-hematite

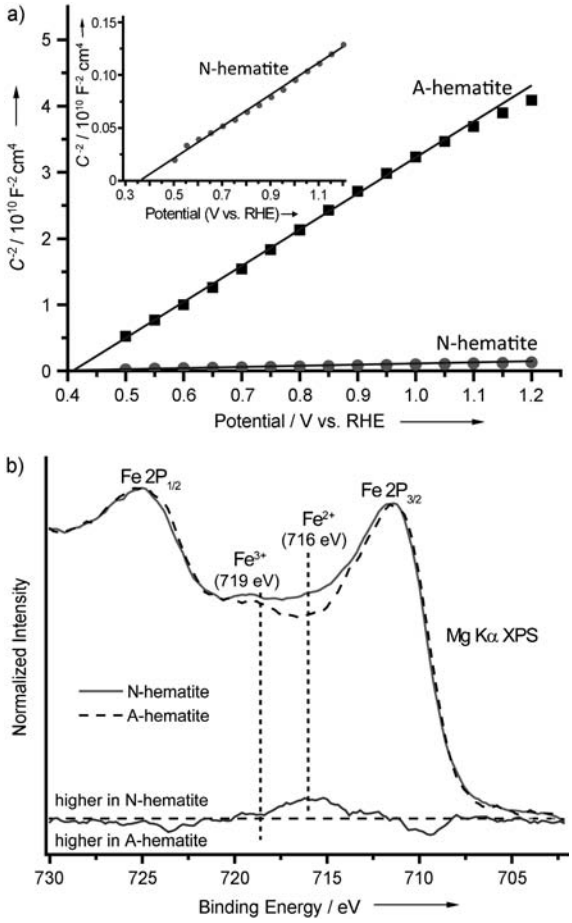

Figure 3. a) Mott–Schottky plots measured for A-hematite (■) and N-hematite (●) nanowire films. The x intercepts of the linear best-fit lines were used to estimate the flat-band potential (V_{FB}). Inset: magnified Mott–Schottky plot of N-hematite. b) Overlay of Fe 2p XPS spectra of A-hematite (-----) and N-hematite (——) films, together with their difference spectrum ("N-hematite" minus "A-hematite"). The vertical dashed lines highlight the satellite peaks for Fe^{3+} and Fe^{2+}.

were measured by Mg K_α XPS (Supporting Information, Figure S3). An estimate of the valence band maximum by linear extrapolation to the baseline leads to band edge positions of approximately 1.60 eV and 1.50 eV below the Fermi energy for N-hematite and A-hematite samples, respectively. The fact that the N-hematite sample exhibits a slightly increased band edge position (vs. A-hematite) indicates an increase in donor density. This result again supports the hypothesis of increased donor density from oxygen vacancy sites and is consistent with the results of the Mott–Schottky studies.

We investigated the mechanism and the influence of oxygen content during thermal treatment on the creation of V_O, and ultimately we were able to control the donor density of hematite. The thermal decomposition of akaganeite to hematite is a critical step, which can be described by the following equation:

$$2\,FeOOH(S) \rightarrow Fe_2O_3(S) + H_2O(g) \quad (5)$$

β-FeOOH is a three-dimensional tunnel structure,[38] which is commonly formed by hydrolysis of $FeCl_3$ in an acidic (pH 1.5) environment. It has been reported that the resulting β-FeOOH typically contains chloride ions and protons in the inner space of the tunnels.[39,40] In an acidic medium, β-FeOOH will uptake protons from solution as shown in the following equation:[39]

$$FeOOH(S) + x\,H^+(aq) \rightarrow FeOOH_{1+x}{}^{x+}(S) \quad (6)$$

To balance the charge, a stoichiometric amount of chloride ions will be captured by the crystal at the same time. The chemical formula of akageneite can then be expressed as $FeOOH_{1+x}Cl_x$. The chloride concentration (x value) varies based on the crystal size and synthetic conditions, such as the pH value.[39–41] The captured chloride ions can be released in the form of hydrogen chloride by reaction with the water molecules produced by dehydroxylation upon thermal treatment at 200 °C or higher. This reaction produces oxygen as a side-product, as shown in the following equation:[38,39]

$$2\,H_2O + 4\,Cl^- \rightarrow 4\,HCl + O_2 + 4\,e^- \quad (7)$$

The oxygen-deficient environment could facilitate the release of hydrogen chloride by shifting the reaction balance towards the right-hand side [Eq. (7)]. We anticipate that the released electrons would reduce Fe^{3+} to Fe^{2+}. Therefore, the thermal decomposition of chloride-containing akaganeite in a N_2 atmosphere can be described as:

$$2\,FeOOH_{1+x}Cl_x(s) \rightarrow Fe_2O_{3-x}(S) + H_2O(g) + 2\,x\,HCl(g) + 0.5\,x\,O_2(g) \quad (8)$$

The O_2 molecules formed as a result of the dehyroxylation of β-FeOOH would be removed by the N_2 gas flow. The formation of a Fe_2O_{3-x} species with V_O and dual-oxidation states (Fe^{2+}/Fe^{3+}) is supported by XPS and Mott–Schottky analysis. In contrast, an oxygen-rich atmosphere, such as air, hinders the release of hydrogen chloride, and akaganeite could be completely converted into α-Fe_2O_3 by the formation of molecular chlorine through the oxidation of chloride by oxygen:

$$2\,FeOOH_{1+x}Cl_x(s) + 0.5\,x\,O_2(g) \rightarrow Fe_2O_3(S) + (0.5+x)\,H_2O(g) + x\,Cl_2(g) \quad (9)$$

Based on the above hypothesis, there are two major parameters in controlling the creation of V_O in hematite: the oxygen content during thermal treatment and the presence of chloride ions. To confirm this hypothesis, we carried out the thermal decomposition of akaganeite at 550 °C for 2 h in three different environments: oxygen-rich (air), oxygen-deficient (N_2 + air) and zero-oxygen (high-purity N_2) atmospheres. Note that the oxygen-rich and deficient environments are the same conditions used for preparing A- and N-hematite samples. To create a zero-oxygen environment, a tube furnace was placed under vacuum to a pressure of < 20 mTorr and then refilled with N_2. This vacuum–fill process was repeated at least three times to ensure that no/minimal air remained in the tube. Akaganeite samples thermally treated in various environments lead to films with different colors (Supporting Information, Figure S4). The A- and N-hematite samples are red, and the sample prepared in the zero-oxygen environment is black. Raman spectra of the two red samples (Figure 4a) can be indexed to the six characteristic Raman peaks of hematite in the range of 200–800 cm^{-1}.[42] However, the intensity of characteristic Raman peaks for hematite are

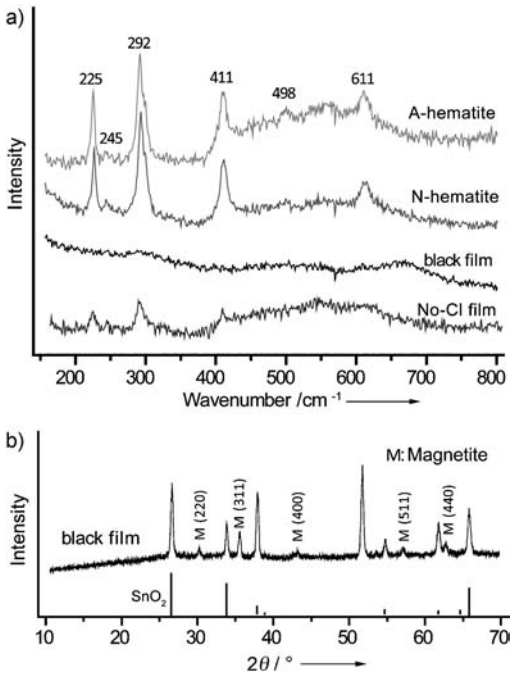

Figure 4. a) Raman spectra of akaganeite samples: thermally treated in air (A-hematite), oxygen-deficient (N_2 + air; N-hematite), N_2 environments (black film), and prepared by a $Fe(NO_3)_3$ precursor solution and thermally treated in N_2 (No-Cl film). b) XRD spectrum collected for the akaganeite samples thermally treated in N_2 at 550 °C. Diffraction peaks labeled with M(hkl) can be indexed to magnetite (JCPDS 19-0629). The lines at the bottom indicate the diffraction peaks of SnO_2 (JCPDS 41-1445) from the FTO substrate.

completely absent in the black sample obtained in the high purity N_2 atmosphere. XRD analysis confirms that the black sample is magnetite (Fe_3O_4) (Figure 4b). Conversion of akaganeite to magnetite has been observed upon thermal decomposition of akaganeite in vacuum.[43] To investigate the role of captured chloride ions in the thermal decomposition of FeOOH into hematite, we prepared FeOOH without chloride ions as a negative control. Chloride-free FeOOH was synthesized under the same conditions, but the $FeCl_3$ precursor solution was replaced with a $Fe(NO_3)_3$ solution. The pH value (1.5) was also adjusted by a HNO_3 solution instead of HCl. FeOOH samples prepared with $FeCl_3$ or $Fe(NO_3)_3$ precursor solutions thermally treated at 550 °C for 2 h in high-purity N_2 atmosphere showed distinct results. In the absence of chloride, the resulting sample is orange instead of black (Supporting Information, Figure S4), and was determined to be hematite by Raman spectroscopy (Figure 4a). To further confirm the effect of chloride ions in the thermal decomposition of akaganeite, we have carried out an additional experiment. The resulting akaganeite samples were put into NaOH solution (0.5 M or 1 M)at 55 °C for 3 h to exchange the Cl^- anions with OH^-.[39] A control experiment where akaganeite was soaked in deionized water at 55 °C for 3 h was carried out in parallel. We thermally treated both anion-exchanged and control samples at 550 °C in a zero-oxygen atmosphere with continuous high-purity N_2 gas flow. As shown in Figure S5 (see the Supporting Information), the samples show different colors after thermal annealing. As expected, the control sample turned black, which indicates the formation of magnetite. In contrast, the anion-exchanged samples (with 0.5 M or 1 M NaOH) are red, which is the typical color for hematite. This experiment again confirms that the Cl^- anions remaining in the akaganeite structure are essential for the creation of Fe^{2+} sites (V_O), and supports the proposed akaganeite–magnetite transformation mechanism.

To summarize, thermal treatment of akaganeite nanowire arrays in an oxygen-deficient environment at 550 °C resulted in significantly improved photoactivity for water oxidation, as compared to samples that were thermally activated in air. The hematite-nanowire-arrayed photoanode yields a photocurrent density of 3.37 mA cm^{-2} at 1.50 V vs. RHE, which is the best value reported to date for pristine hematite materials without the incorporation of dopants or oxygen-evolving catalysts. The enhancement in photoactivity is because of the increased donor density resulting from the formation of V_O (Fe^{2+}). The presence of chloride ions and an oxygen-deficient environment are essential for the creation of V_O. This work demonstrated a simple and effective method for the preparation of highly photoactive hematite for use in PEC water oxidation, without the need for dopants and at a relatively low activation temperature.

Received: October 23, 2011
Revised: January 10, 2012
Published online: March 13, 2012

Keywords: hematite · nanowires · oxygen vacancies · photochemistry · water splitting

[1] H. L. Wang, J. A. Turner, *J. Electrochem. Soc.* **2010**, *157*, F173.
[2] Y. Ling, G. Wang, D. A. Wheeler, J. Z. Zhang, Y. Li, *Nano Lett.* **2011**, *11*, 2119.
[3] K. Sivula, F. Le Formal, M. Grätzel, *ChemSusChem* **2011**, *4*, 432.
[4] S. D. Tilley, M. Cornuz, K. Sivula, M. Grätzel, *Angew. Chem.* **2010**, *122*, 6549; *Angew. Chem. Int. Ed.* **2010**, *49*, 6405.
[5] Y. Lin, S. Zhou, S. W. Sheehan, D. Wang, *J. Am. Chem. Soc.* **2011**, *133*, 2398.
[6] G. Wang, H. Wang, Y. Ling, Y. Tang, X. Yang, R. C. Fitzmorris, C. Wang, J. Z. Zhang, Y. Li, *Nano Lett.* **2011**, *11*, 3026.
[7] A. Fujishima, K. Honda, *Nature* **1972**, *238*, 37.
[8] Y. Lin, S. Zhou, X. Liu, S. Sheehan, D. Wang, *J. Am. Chem. Soc.* **2009**, *131*, 2772.
[9] Y. J. Hwang, A. Boukai, P. Yang, *Nano Lett.* **2009**, *9*, 410.
[10] X. Feng, K. Shankar, O. K. Varghese, M. Paulose, T. J. Latempa, C. A. Grimes, *Nano Lett.* **2008**, *8*, 3781.
[11] G. M. Wang, X. Y. Yang, F. Qian, J. Z. Zhang, Y. Li, *Nano Lett.* **2010**, *10*, 1088.
[12] R. Solarska, A. Krolikowska, J. Augustynski, *Angew. Chem.* **2010**, *122*, 8152; *Angew. Chem. Int. Ed.* **2010**, *49*, 7980.
[13] J. Z. Su, X. J. Feng, J. D. Sloppy, L. J. Guo, C. A. Grimes, *Nano Lett.* **2011**, *11*, 203.
[14] J. Z. Su, L. J. Guo, N. Z. Bao, C. A. Grimes, *Nano Lett.* **2011**, *11*, 1928.
[15] R. Liu, Y. Lin, L.-Y. Chou, S. W. Sheehan, W. He, F. Zhang, H. J. M. Hou, D. Wang, *Angew. Chem.* **2011**, *123*, 519; *Angew. Chem. Int. Ed.* **2011**, *50*, 499.
[16] N. J. Cherepy, D. B. Liston, J. A. Lovejoy, H. M. Deng, J. Z. Zhang, *J. Phys. Chem. B* **1998**, *102*, 770.
[17] M. P. Dareedwards, J. B. Goodenough, A. Hamnett, P. R. Trevellick, *J. Chem. Soc. Faraday Trans.* **1983**, *79*, 2027.
[18] I. Cesar, K. Sivula, A. Kay, R. Zboril, M. Graetzel, *J. Phys. Chem. C* **2009**, *113*, 772.
[19] K. Sivula, R. Zboril, F. Le Formal, R. Robert, A. Weidenkaff, J. Tucek, J. Frydrych, M. Grätzel, *J. Am. Chem. Soc.* **2010**, *132*, 7436.
[20] M. G. Walter, E. L. Warren, J. R. McKone, S. W. Boettcher, Q. X. Mi, E. A. Santori, N. S. Lewis, *Chem. Rev.* **2010**, *110*, 6446.
[21] D. K. Zhong, M. Cornuz, K. Sivula, M. Grätzel, D. R. Gamelin, *Energy Environ. Sci.* **2011**, *4*, 1759.
[22] D. K. Zhong, D. R. Gamelin, *J. Am. Chem. Soc.* **2010**, *132*, 4202.
[23] D. K. Zhong, J. W. Sun, H. Inumaru, D. R. Gamelin, *J. Am. Chem. Soc.* **2009**, *131*, 6086.
[24] J. Brillet, M. Grätzel, K. Sivula, *Nano Lett.* **2010**, *10*, 4155.
[25] M. Zhang, W. Luo, Z. Li, T. Yu, Z. Zou, *Appl. Phys. Lett.* **2010**, *97*, 042105.
[26] N. Iordanova, M. Dupuis, K. M. Rosso, *J. Chem. Phys.* **2005**, *122*, 144305.
[27] C. Castro, L. Oliveira, M. Guerreiro, *Catal. Lett.* **2009**, *133*, 41.
[28] L. Vayssieres, N. Beermann, S. E. Lindquist, A. Hagfeldt, *Chem. Mater.* **2001**, *13*, 233.
[29] R. Morrish, M. Rahman, J. M. D. MacElroy, C. A. Wolden, *ChemSusChem* **2011**, *4*, 474.
[30] A. Kay, I. Cesar, M. Grätzel, *J. Am. Chem. Soc.* **2006**, *128*, 15714.
[31] A. Duret, M. Grätzel, *J. Phys. Chem. B* **2005**, *109*, 17184.
[32] R. van de Krol, M. Grätzel, *Photoelectrochemical Hydrogen Production*, Springer, New York, **2011**, p. 147.
[33] T. Fujii, F. M. F. de Groot, G. A. Sawatzky, F. C. Voogt, T. Hibma, K. Okada, *Phys. Rev. B* **1999**, *59*, 3195.
[34] G. Wang, Y. Ling, D. A. Wheeler, K. E. N. George, K. Horsley, C. Heske, J. Z. Zhang, Y. Li, *Nano Lett.* **2011**, *11*, 3503.
[35] K. Wandelt, *Surf. Sci. Rep.* **1982**, *2*, 1.
[36] J. F. Moulder, W. F. Stickle in *Physcial Electronics Division*, PerkinElmer Coporation, Eden Prairie, MN, **1992**.

[37] V. M. Aroutiounian, V. M. Arakelyan, G. E. Shahnazaryan, H. R. Hovhannisyan, H. Wang, J. A. Turner, *Sol. Energy* **2007**, *81*, 1369.
[38] E. Paterson, R. Swaffield, D. R. Clark, *Thermochim. Acta* **1982**, *54*, 201.
[39] J. Cai, J. Liu, Z. Gao, A. Navrotsky, S. L. Suib, *Chem. Mater.* **2001**, *13*, 4595.
[40] K. Ståhl, K. Nielsen, J. Jiang, B. Lebech, J. C. Hanson, P. Norby, J. van Lanschot, *Corros. Sci.* **2003**, *45*, 2563.
[41] K. M. Parida, *J. Mater. Sci.* **1988**, *23*, 1201.
[42] D. L. A. de Faria, S. Venâncio Silva, M. T. de Oliveira, *J. Raman Spectrosc.* **1997**, *28*, 873.
[43] M. D. Meroño, J. Morales, J. L. Tirado, *Thermochim. Acta* **1985**, *92*, 525.

